Global limits on CO_2 geological storage deployment using a coupled industry growth - pressure constrained model

Iain de Jonge-Anderson[*1], Gareth Johnson[2], Juan Alcalde[3] & Jennifer J. Roberts[1]

[1]Department of Civil & Environmental Engineering, University of Strathclyde, Glasgow, UK
[2]Drax Group, Drax Power Station, Selby, North Yorkshire, UK
[3]Geosciences Barcelona (GEO3BCN), CSIC, Barcelona, Spain
*Corresponding author (email: iain.de-jonge-anderson@strath.ac.uk)
ORCiDs: 0000-0002-9438-8194 (IdJA)
0000-0003-4505-8524 (JJR)
0000-0002-3151-5045 (GJ)
0000-0001-9806-5600 (JA)

Abstract

Geological storage of CO_2 at scale is critical to meeting climate objectives, yet deployment targets often rely on top-down climate pathways that overlook the coupled constraints of subsurface pressure buildup and realistic industry drilling rates. Here we map global limits on CO_2 storage deployment using CO2LOGIX 2.0, an improved model coupling subsurface pressure evolution with country-level deployment trajectories. We model nine scenarios, varying which countries participate and how quickly they scale, informed by volumes stored to date, historical drilling rates, project pipelines and storage readiness indicators. We find near-term global injection rates are significantly lower than previous estimates, reaching 2.71 $GtCO_2yr^{-1}$ by 2050 and peaking at 56.45 $GtCO_2yr^{-1}$ under central assumptions. Halving growth rates and extending start-up delays reduces the 2050 and peak rates to 0.35 and 32.7 $GtCO_2yr^{-1}$; increasing growth rates by half and shortening delays gives 16.6 and 70.7 $GtCO_2yr^{-1}$. Near-term expansion is driven by early adopters such as the USA and Brazil, while later expansion concentrates in China, Saudi Arabia, India and Southeast Asia. Cumulative storage by 2100 exceeds almost all 1.5 °C mitigation pathways, but near to mid-term projections appear overestimated – a mismatch that persists across every modelled scenario. Greater volumes could be achieved by targeting countries whose potential remains untapped even under the most aggressive scale-up assumptions, concentrated in sub-Saharan Africa, the Middle East and South America. This is the first study to constrain global injection rates with a coupled industry growth-pressure model, offering an adaptable framework for evaluating CO_2 geological storage deployment.

Keywords

CO_2 storage capacity; Injectivity; CCS growth; Pressure response; Simplified models

1. Introduction

CO_2 geological storage (CGS) is regarded as an essential technology for limiting climate change and climate mitigation scenarios typically project Gigatonne-scale deployment. Pathways meeting 1.5°C with no or limited overshoot (C1) submitted to IPCC's Sixth Assessment Report database (Byers et al., 2022) projected median injection rates of 7.82 $GtCO_2yr^{-1}$ by 2050 and 14.50 $GtCO_2yr^{-1}$ by 2100. Similarly, the IEA's Net Zero Emissions by 2050 Scenario includes the expansion of capture rates to 6.05 $GtCO_2yr^{-1}$ by 2050 (IEA, 2025). Realising these projections would require a vast and rapid scale-up of the CGS industry, which in 2023 accounted for only 0.045 $GtCO_2yr^{-1}$ (Gao & Krevor, 2025).

Studies utilising technoeconomic growth modelling have suggested feasible upper limits for CGS industry scale-up. Kazlou et al. (2024) demonstrated that a feasible pathway could consist of 0.37 $GtCO_2yr^{-1}$ by 2030 and up to 4.3 $GtCO_2yr^{-1}$ by 2040; however, note that even the 2030 target would require an eight-fold increase in six years from the latest (2023) storage volume achieved (Gao & Krevor, 2025). Zhang et al. (2024) further suggested a feasible 2050 benchmark of 5-6 $GtCO_2yr^{-1}$ globally. While these studies account for the capture capacity reported for active and planned projects, historical rates of technology adoption, national storage ambitions and total storage resource, no previous study considers one of the fundamental controls on CGS scale-up: the interplay between technology growth and dynamic subsurface behaviour (Lane et al., 2021).

Among the potential subsurface limits on CGS scale-up, the pressure response in saline aquifers is of critical importance. In saline aquifer storage, CO_2 is introduced into a porous volume already saturated with brine at hydrostatic pressure. CO_2 injection, migration and storage are accommodated by the compressibility of the rock and fluids, as well as the mobility of brine; however, the ease with which these mechanisms occur depends on geological factors such as the connectivity of the storage formation and boundary conditions (Worden, 2024). The resulting brine displacement and compression of the rock-fluid system leads to an increase in pore fluid pressure throughout the affected subsurface volume. Injection projects have demonstrated that near-well fluid pressure can, in some instances, rise quickly and unexpectedly (Hansen et al., 2013; Shi et al., 2019) while at the basin scale, modelling studies indicate that pressure fronts can propagate tens of kilometres away from the injection zone and persist for hundreds of years (Birkholzer & Zhou, 2009; De Luca et al., 2025; Thibeau et al., 2014). As CGS projects typically operate within strict pressure limits, pressure can be conceptualised as a finite resource (Bump & Hovorka, 2024) that is depleted as the limit is approached. Consequently, understanding the degree to which pressure increases during and after injection is imperative, not only for evidencing the safety and viability of individual projects during permitting, but also for accurately characterising the storage portfolios of entire nations and regions.

Pressure availability is also a dynamic problem that is highly sensitive to how the industry develops: specifically, the rate at which new injection wells are drilled and their spatial distribution determines how rapidly and where pressure constraints emerge and ultimately how much of the storage resource can be utilised over time. Smith et al. (2024) calculated global pressure-limited CGS capacity using the CO2BLOCK pressure analytical framework (De Simone & Krevor, 2021), and estimated a capacity of 5,630 $GtCO_2$, over seven times greater than the storage requirements in most IPCC climate change mitigation pathways (Byers et al., 2022). While the Smith et al. (2024) estimate accounts for pressure interference across injection sites and injectivity constraints it assumes full and immediate utilisation of the potential storage portfolio of each country, thereby providing an upper bound irrespective of scale-up limitations. To address this, de Jonge-Anderson et al. (2026) coupled the same pressure analytical function used in CO2BLOCK with a logistic growth model (CO2LOGIX 1.0) to explore how growth trajectory impacts pressure limits and storage constraints, limited to a UK exemplar. However, there remains a need to consider global constraints on CGS deployment, accounting for different degrees of geographical participation in pursuing CGS, scale-up rates across different nations and the geological characteristics of their national storage resource. Constraining CGS deployment is particularly paramount for Integrated Assessment Models (IAMs) that rely on such datasets to inform climate change mitigation pathways and ensure that policy-facing outputs and reports are feasible and reflect the latest scientific understanding. In this study, we address this need by evolving CO2LOGIX and deploying it at a global scale to assess limits on storage potential and injectivity and, ultimately, to provide a physically grounded envelope of feasible deployment against which the storage assumptions embedded in climate mitigation pathways can be tested.

2. Methodology

2.1. The CO2LOGIX model

The core modelling framework used within this study, CO2LOGIX, is a computationally efficient, first-order model designed to simulate basin-scale pressure evolution during CO_2 injection into deep saline aquifers under different industry deployment scenarios (de Jonge-Anderson et al., 2026). It couples subsurface dynamics with industry growth trajectories, represented by the evolution of drilling rates, enabling the assessment of pressure-constrained storage capacity over time. CO_2 injection wells are randomly distributed across the model domain. The model domain could be as granular as an individual storage formation, an entire basin, or multiple basins. The choice of modelling domain is driven by the data available and modelling scope. Averaged geological properties (including permeability, porosity, thickness, and depth) are then assigned to each formation within that domain.

The CO2LOGIX framework consists of two distinct components, described below: (1) a logistic growth model that describes the temporal deployment of injection wells, and (2) an analytical pressure model that estimates pressure buildup resulting from CO_2 injection.

2.1.1. Growth model and well deployment

The temporal evolution of CGS deployment is represented using a logistic growth function, used to define the cumulative number of injection wells as a function of time. The S-shape morphology of the logistic growth function approximates typical phases of technology deployment, from initial (slow) uptake, through (rapid) expansion, to eventual saturation. It is parameterised by three variables: the carrying capacity (maximum number of injection wells the region can accommodate), the growth rate, and the year at which growth reaches its peak (midpoint year). At each (yearly) timestep, the logistic growth model determines the number of new wells introduced into the system. In CO2LOGIX 1.0, each well was assigned a fixed injection rate of 1 $Mtyr^{-1}$ and an operational life of 25 years (de Jonge-Anderson et al., 2026), however, in CO2LOGIX 2.0, we introduce injection rates that scale with geological properties (see Section 2.1.3).

2.1.2. Pressure simulation

Once CO_2 injection starts, the pressure buildup per well is calculated using the analytical solution of Nordbotten et al. (2005), closely mirroring the implementation also adopted in CO2BLOCK (De Simone et al., 2019; De Simone & Krevor, 2021; Kivi et al., 2025; Smith et al., 2024). For each actively injecting well at a given timestep, pressure is computed as a function of injection rate, reservoir properties, and time since injection commenced. The analytical solution assumes radial pressure diffusion, with pressure decreasing logarithmically with distance from the well and propagating outward over time.

At the end of each timestep, pressure contributions from each actively injecting well are superposed to approximate pressure interference and generate basin-scale pressure buildup. Simulated pressure is then normalised relative to an estimate of fracture pressure based on an empirical relationship (Zhang & Yin, 2017), allowing comparison across formations with different depths and stress conditions. A maximum allowable pressure threshold is imposed, approximating operational or regulatory limits. CO2LOGIX 1.0 (de Jonge-Anderson et al., 2026) did not respond in any way to a breach of the pressure limit, but in CO2LOGIX 2.0, we introduce shut-down logic to avoid pressure buildup beyond the limit specified (see Section 2.1.3).

2.1.3. Improvements to the pressure model in CO2LOGIX 2.0

There are two key limitations to the pressure model component of CO2LOGIX 1.0 which we address in this study: (i) the uniform injection rate of 1 $Mtyr^{-1}$ irrespective of storage formation characteristics, and (ii) the continued injection after the defined pressure limit is reached. We address these two limitations with two structural changes. In CO2LOGIX 2.0 we introduce variable injection rates linked to storage formation characteristics and logic that stops wells injecting once a local pressure limit is reached.

Geologically informed CO_2 injection rates

We introduce modelled injection rates that are scaled according to the geological properties of the storage unit, allowing well performance to vary realistically between storage formations. The rates are estimated based on the storage formation's average permeability (κ) and thickness (h). Valluri et al. (2021) examined injectivity data from ten active CGS projects and established an empirical correlation between injectivity index (J) and the product of permeability and thickness (κh):

$$J = \alpha \kappa h \qquad \text{Eq. 1}$$

Where J is the injectivity index in t/yr/psi, κ is permeability (mD) and h is thickness (ft). The mean fitting parameter derived by Valluri et al (2021) (α) was 0.08, with a lower bound of 0.03 and an upper bound of 0.23. We adopt the lower bound in this work as a conservative estimate, while noting that using the mean or upper bound would result in greater injection rates across all modelled wells. We convert the units of the fitting parameter (to express

J in t/yr/MPa and h in metres) to give corresponding α values of 38 (mean), 14 (lower) and 109 (upper). Following this, we calculate CO_2 injection rate (in $Mtyr^{-1}$) as:

$$I = \Delta P_{allowable} J \qquad \text{Eq. 2}$$

Where $\Delta P_{allowable}$ is the allowable pressure increase, defined as the difference between hydrostatic and 80% of fracture pressure. Finally, we impose an upper limit of 2 $Mtyr^{-1}$ to avoid unrealistically high injection rates.

Functionality to shut in wells

In CO2LOGIX 2.0, we introduce logic that halts injection and shuts in (prematurely closes) wells if the defined local pressure threshold is breached. When a well is shut in, further injection ceases and its pressure contribution is frozen, reflecting real-world operational curtailment. To do this, we use a search function limited to locations within the pressure influence radius of each well. If the pressure limit is breached anywhere within that well's influence radius, the well that is injecting is removed from subsequent timesteps and its pressure response frozen (i.e. no pressure dissipation is considered).

Introducing injection well shut in logic removes the requirement to terminate the simulation and define the final storage capacity at the year the pressure limit is reached (de Jonge-Anderson et al., 2026). Instead, the simulation continues by successively removing wells that exceed the defined pressure limit, allowing storage capacity to emerge dynamically over time rather than being constrained by the first occurrence of pressure limit exceedance.

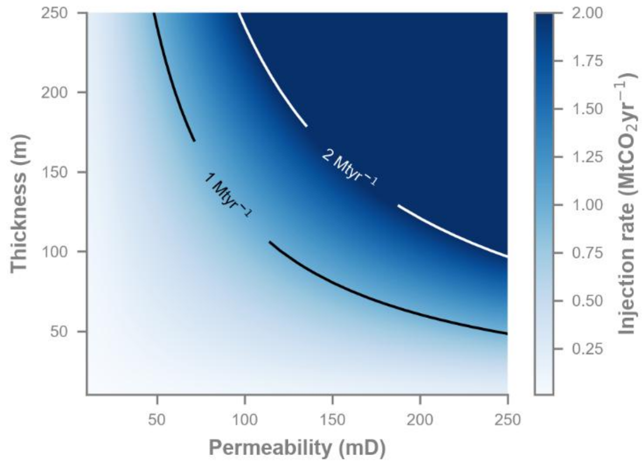

Figure 1: A surface plot highlighting how permeability and thickness translate to injection rate following the empirical relationship of Valluri et al. (2021). We adopt the conservative coefficient of 0.03 described in Valluri et al. (2021). An upper limit of 2 $Mtyr^{-1}$ per well is enforced to ensure that injection rates remain reasonable even for highly permeable, thick formations.

2.1.4. Key model limitations

While CO2LOGIX 2.0 introduces key improvements, several important limitations remain and warrant discussion. Firstly, we treat storage formations as single, regional saline aquifer storage units. The model does not consider multi-layered or stacked saline aquifer systems where vertical pressure communication or multi-zone injection could aid pressure management and improve injectivity (Bump et al., 2023).

Secondly, CO2LOGIX 2.0 still assumes persistent pressure buildup without active pressure management interventions (such as brine extraction via production wells). Implementing active pressure management could delay local pressure limit exceedance, potentially reducing the well shut-in rates and lost capacities observed in high-density deployment scenarios.

2.2. The global geological model: parameters and assumptions

The parameters used in the global-scale deployment of CO2LOGIX 2.0 are shown in Table 1. We use a database of basin-averaged reservoir properties covering 203 sedimentary basins (Smith et al., 2024) (Figure 2). The Smith et al. (2024) database represents the most complete account of geological properties globally, spanning 71 countries and including many of the most important geological basins for CGS. However, the Smith et al. (2024) database covers only a subset of the 764 sedimentary basins mapped globally (Evenick, 2021); the necessary geological properties (porosity, permeability, depth and thickness) are not defined for the remaining basins, and are therefore not modelled here. To obtain country-level data on basin geological properties we create a shapefile per country by first filtering the database on the “Majority Country” field before joining it to the geospatial dataset of Evenick (2021).

We use further inputs where appropriate and retain the functionality to add extra datasets in future CO2LOGIX versions. For example, rather than using Smith et al. (2024) data for the UK, we use the saline aquifers published previously in de Jonge-Anderson et al. (2026) (Figure 2) as these are derived from a more comprehensive set of studies. Furthermore, given the USA dataset of Smith et al. (2024) does not include key basins such as the Gulf of Mexico, we instead use a different USA dataset produced by Pett-Ridge et al. (2023) (Figure 2).

Bringing these datasets together, we create a modelling domain spanning 29% of all global sedimentary basins by area. The breakdown by country is variable. By area, 72% of all sedimentary basins in China are represented, yet the coverage falls to 42% and 31% for Brazil and USA, two countries with strong CGS ambitions. This partial coverage reflects the state of published geological resource assessments rather than a limitation of this modelling work, and basins without assessed properties can only add resource - so the capacities modelled here are a lower bound. Coverage is concentrated where deployment is actually happening, with the modelled countries accounting for 97% of all CO_2 stored to date (Gao & Krevor, 2025), and further assessments can be incorporated as they are published, as we have done for the UK and USA.

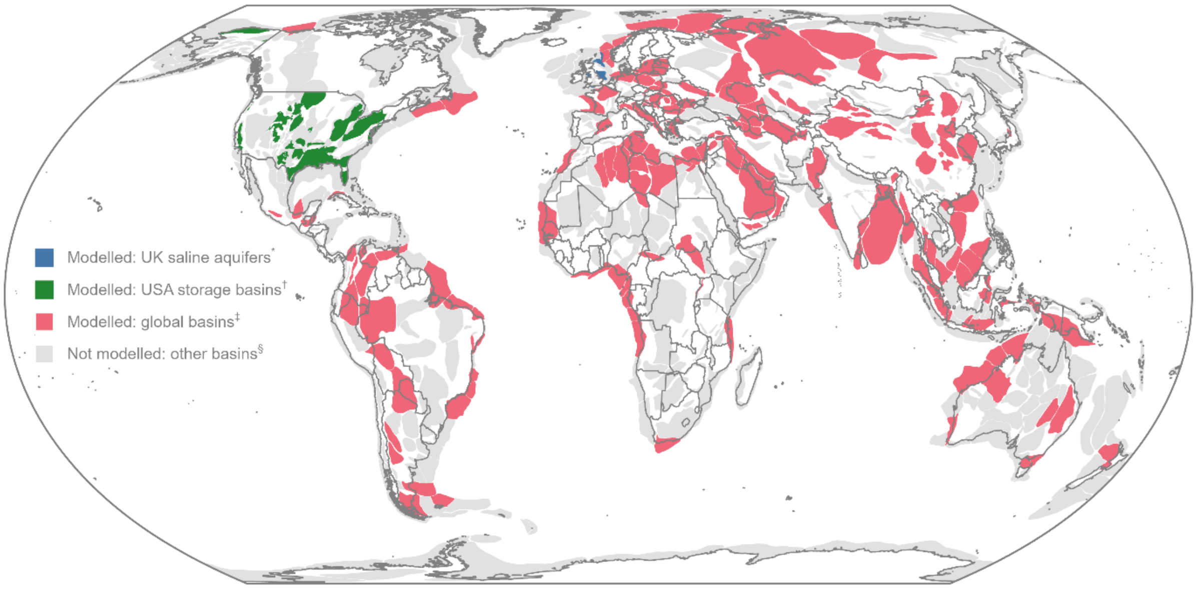

*Figure 2: Distribution of storage units modelled in this study relative to all sedimentary basins globally. * de Jonge-Anderson et al. (2026), † Pett-Ridge et al. (2023), ‡ Smith et al. (2024), § Evenick (2021).*

We calculate several intermediate parameters including total compressibility and fracture pressure using first-order relationships derived from the literature (Table 1). It is important to emphasise that these represent estimates that would need to be refined at a local scale for more accurate predictions. Each well in the global simulation injects for 25 years (reflecting the typical well lifespan of a commercial injection project (Smith et al., 2025)) at the injection rate scaled to κh as described in Section 2.1.3, unless the pressure limit is breached. The wells are placed at random geographical locations within each basin, but with an area-based weighting to ensure that a proportional number of wells are assigned to each basin (i.e. more wells are placed in larger basins in a given country). The amount of CO_2 stored in each basin is tracked, and if a basin reaches its pressure-limited storage capacity, subsequent wells allocated to that basin are relocated to a basin within the same country with remaining capacity. Once no remaining storage capacity is available across any basin within a country, no further wells are added for that country.

Category	Parameter	Definition
Wells	Injection rate	Informed by product of permeability and thickness (after Valluri et al. (2021))
	Lifetime	25 years
	Pressure limit	80% of fracture pressure
	Maximum per country	Pressure space capacity / injection rate / lifetime
	Location	Random xy coordinates in basin(s)
Saline aquifer	Porosity	Basin-averaged (Pett-Ridge et al., 2023; Smith et al., 2024) or saline aquifer-averaged (de Jonge-Anderson et al., 2026)
	Permeability	Basin-averaged (Pett-Ridge et al., 2023; Smith et al., 2024) or saline aquifer-averaged (de Jonge-Anderson et al., 2026)
	Compressibility	Derived empirically from porosity (Newman, 1973)

	Depth	Basin-averaged (Pett-Ridge et al., 2023; Smith et al., 2024) or saline aquifer-averaged (de Jonge-Anderson et al., 2026)
	Thickness	Basin-averaged (Pett-Ridge et al., 2023; Smith et al., 2024) or saline aquifer-averaged (de Jonge-Anderson et al., 2026)
	Initial pressure	Hydrostatic, at 10 MPa/km
	Fracture pressure	Pore pressure plus 0.75 x (vertical pressure - pore pressure) (Zhang & Yin, 2017)
Simulation	Grid size	1000 m

Table 1: Parameters used in the global-scale deployment of CO2LOGIX 2.0 and how each is defined.

2.3. How deployment and scale-up assumptions are modelled

We use logistic growth models to constrain the number of simulated CO_2 injection wells per country per year. Constraining such models for countries at different stages of economic development and with different capability to develop a CGS industry can be challenging. Nevertheless, several studies have demonstrated that logistic growth models can be an effective tool in considering the deployment of negative emissions technologies (Edwards et al., 2024; Nemet et al., 2023), including CGS (Fuhrman et al., 2025; Zhang et al., 2024). However, these studies are focused primarily on technoeconomic drivers of CGS, where the models are constrained based on volumes of CO_2 stored over time. Our study is distinct from these by coupling logistic growth trajectories with subsurface pressure evolution, which allows growth to be constrained by drilling rates rather than CO_2 storage volumes, as the latter are an output of CO2LOGIX rather than an input.

We use four mechanisms to constrain and parameterise individual growth trajectories per country (Figure 3):

a) Carrying capacity, informed by pressure-constrained storage potential (Figure 3a).
b) Logistic growth rate, informed by historical drilling rates and scaled to storage readiness (Figure 3b).
c) Midpoint year, informed by known storage volumes in 2023 (Figure 3c).
d) A start delay, informed by storage readiness and the delay observed in the UK (Figure 3d).

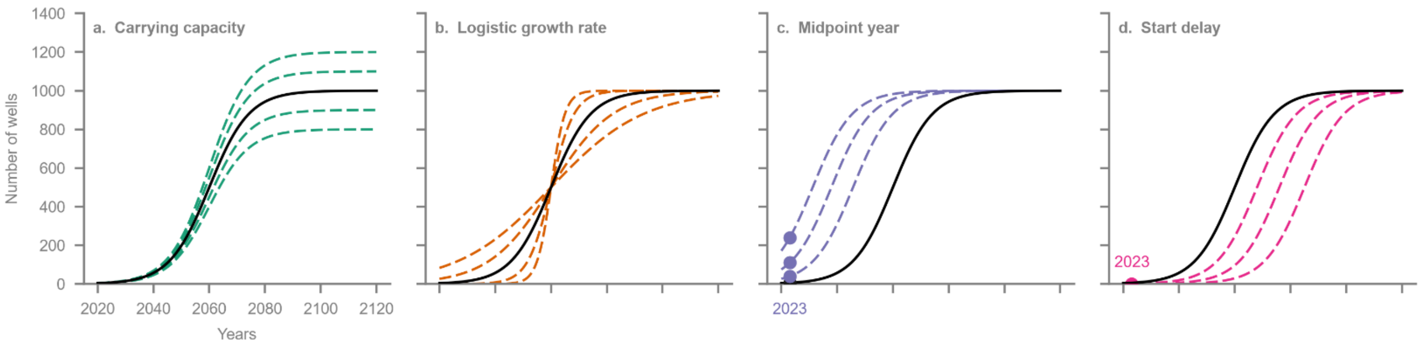

Figure 3: Schematic illustrations of the logistic growth function used to calculate drilling rates for input to CO2LOGIX. a: the carrying capacity (L) is determined from the pressure-constrained storage potential and the number of wells required to fully utilise that potential. It controls the y-scale of the curve. b: the logistic growth rate (k) is informed by historical drilling rates and scaled according to a country's readiness to deploy CGS. It controls how steep the curve is at its inflection point. c: the midpoint year (t_m) is solved for endogenously using the deployment level in 2023 and the other logistic growth parameters. It controls the x-scale of the curve. d: the start delay controls the year at which the growth function begins. It is informed by storage readiness and the actual delay in deploying CGS in the UK.

We describe the rationale and implementation for each mechanism in turn.

Carrying capacity

We adopt the methodology of de Jonge-Anderson et al. (2026) in estimating the carrying capacity per country. Pressure-constrained storage potential is first estimated using the method outlined in Bump and Hovorka (2024), based on the pore volume, allowable pressure increase, total compressibility and in situ CO_2 density of each saline aquifer. We then estimate how many injection wells would be required to fully utilise this potential, using geologically informed injection rates (see Section 2.1.3) and an assumed 25-year lifetime per well. The total well count is then set to the carrying capacity of the logistic function (Figure 3a).

Logistic growth rate

To establish a representative range of growth rates for drilling capacity, we utilise historical data on hydrocarbon drilling rates from the United Kingdom Continental Shelf (released by the North Sea Transition Authority), Gulf of Mexico, Texas and Norway (Ringrose & Meckel, 2019) (Figure 4). We fitted logistic growth functions to these datasets and found that the growth rate (k) varies only marginally from 10% (Gulf of Mexico) to 15% (Texas) (Figure 4). Because these rates are consistent across different geological basins and regulatory regimes, and agree closely with the 13% median logistic growth rate reported for a wide range of technologies (Nemet et al., 2023), we consider them representative of achievable growth in drilling rates for a developing CGS industry.

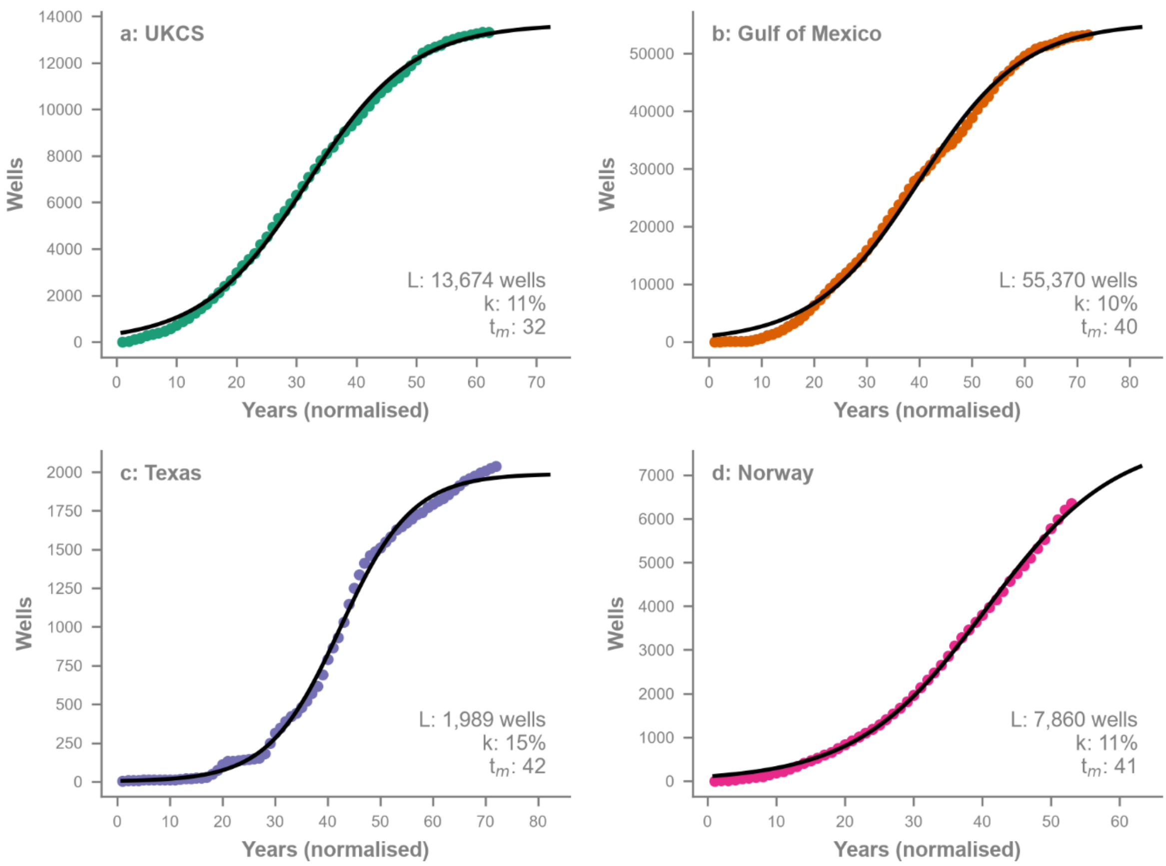

Figure 4: Annual wells drilled in four regions. a: United Kingdom Continental Shelf (UKCS), b: Gulf of Mexico, c: Texas and d: Norway. The x-axis is normalised to ease comparison between regions. A logistic growth function (solid line) is fitted to each set of data points and the fitted parameters noted in the relevant panel. Note that while the carrying capacity (L) varies substantially across regions, their growth rates (k) and midpoint years (t_m) are relatively consistent at 10-15% and 32-42 respectively.

To represent differences among countries in their readiness to deploy CGS, we define a classification scheme (Table 2) based on volumes stored to-date (Gao & Krevor, 2025), the presence of planned projects (IEA, 2026), storage readiness as defined by the Global CCS Institute (Consoli, 2018) and the availability of basic geological information on storage characteristics (Smith et al., 2024). We assign countries already deploying CGS at scale a growth rate of 15%, corresponding to the upper bound observed in the historical drilling datasets (Figure 4), while countries with evidence of committed/announced projects are assigned 10%, corresponding to the lower bound. For less mature categories, where no empirical drilling trajectory is available, we progressively reduce the assumed growth rate: countries that have appraised their storage resources but are not planning projects yet are assigned a growth rate of 7.5%, while countries with no strong evidence of readiness to start CGS deployment ("Conceptual") are assigned 5% (Table 2).

Class	Qualifiers	Countries	Assigned growth rate (%)	Assigned injection delay (years)	Scenarios included within
Injecting	Evidence of injection at scale and/or Operational projects	Australia, Brazil, Canada, China, Croatia, Hungary, Norway, Saudi Arabia, USA (n=9)	15	none	All: Limited, Reference and Maximum
Pipeline	Committed or announced project	France, Greece, India, Indonesia, Italy, Japan, Libya, Malaysia, New Zealand, Oman, Papua New Guinea, Poland, Romania, Russia, Spain, Thailand, UK (n=17)	10	10	
Appraised	No projects, but resource assessed and Storage Readiness defined	Algeria, Angola, Austria, Egypt, Germany, Iran, Israel, Kazakhstan, Latvia, Mexico, Morocco, Myanmar, Nigeria, Pakistan, Philippines, South Africa, Tunisia, Turkey, Vietnam (n=19)	7.5	25	Reference and Maximum
Conceptual	No injection, projects, appraisal of Storage Readiness but geological data available	Argentina, Azerbaijan, Belize, Bolivia, Cameroon, Chad, Colombia, Cote d'Ivoire, Cuba, Falkland Islands, Gabon, Ghana, Iraq, Peru, Senegal, Sudan, Syria, Tajikistan, Tanzania, Trinidad and Tobago, Turkmenistan, Uganda, Ukraine, Uzbekistan, Venezuela, Yemen (n=26)	5	50	Maximum

Table 2: Classification scheme used to assign growth rate and injection delays to different countries according to their readiness to deploy CGS, based on Consoli (2018), Gao and Krevor (2025) and IEA (2026).

Start delay

We use the classification scheme (Table 2) to enforce an informed delay on the first year a country starts injecting CO_2, designed to reflect the different ambitions and readiness of different countries in developing a CGS industry. These delays are intended as first-order assumptions that progressively increase with decreasing deployment readiness, rather than empirically determined development timescales. Countries already injecting CO_2 are assigned no delay, while those with planned projects are assigned a 10-year delay reflective of conservative lead times to get projects from announced to injecting (ZEP, 2010) (Table 2).

A delay of 25 years is assigned to countries where storage resources have been formally assessed but where no development projects are presently identified. The UK provides an illustrative example, with approximately 24 years passed between when CCS was first identified as a "promising way forward" in 2003 (Waring & Longo, 2025) and the expected start-up of its first commercial-scale storage project, Endurance (2027) (NSTA, 2024). Finally, we assign a 50-year delay to countries that show no evidence of planned projects or significant appraisal of their resources.

Midpoint year

The midpoint year is calculated endogenously using known volumes of CO_2 stored and the other logistic parameters (carrying capacity and growth rate). To estimate the number of injection wells operating in each country, we use the London Register of Subsurface CO_2 Storage (Gao & Krevor, 2025), which provides the latest published complete record of reported storage volumes. The latest full year in the register is 2023; we therefore use 2023 as the starting point for the simulation. To convert the reported volumes stored (as described in Gao and Krevor (2025)) to an equivalent number of wells, we divide the volume by the mean injection rate estimated within CO2LOGIX (see Section 2.1.3). If a country is not present in the database, we assume that its CGS deployment starts from a very low base, represented by a single injection well in its first year of deployment.

2.4. Overview of scenarios modelled

We run CO2LOGIX 2.0 across nine distinct scenario combinations, evaluating three deployment scenarios (which govern geographical participation) across three scale-up assumptions (which govern the pace of industry expansion) (Table 3). The full list of countries and parameters can be found in the Supplementary Data to this article. The deployment scenarios determine which countries participate in CGS, while the scale-up assumptions determine how rapidly deployment proceeds within those countries. Our baseline case combines *Reference* deployment with *Central* scale-up *(Reference (Central)*). Here, all countries within the “Injecting”, “Pipeline” and “Appraised” categories are modelled using the growth rates assigned to them in Table 2. We consider this to be the most pragmatic pathway for future deployment. We also consider two further deployment scenarios: *Limited*, in which only “Injecting” and “Pipeline” countries pursue CGS (26 countries) and *Maximum*, in which all 71 countries included in the model, including those classified as “Appraised” and “Conceptual”, pursue CGS. The results of these modelling runs are presented in Section 3.1.

For each deployment scenario, we also consider *Slow*, *Central* and *Fast* scale-up assumptions. We use simple multipliers to modify the assigned growth rates and start delays. Under *Fast* scale-up, growth rates are increased by 50% (×1.5) and delays reduced by 50% (×0.5). Under *Slow* scale-up, growth rates are reduced by 50% (×0.5) and delays increased by 50% (×1.5); the *Central* case retains the values defined in Table 2. The results of these modelling runs are presented in Section 3.2.

Deployment scenario	Scale-up assumption	Scenario abbreviation	Participating countries (n)	Growth rate multiplier	Delay multiplier
Limited	Slow	*Limited (Slow)*	26	x 0.5	x 1.5
Limited	Central	*Limited (Central)*	26	Baseline	Baseline
Limited	Fast	*Limited (Fast)*	26	x 1.5	x 0.5
Reference	Slow	*Reference (Slow)*	45	x 0.5	x 1.5
Reference	Central	*Reference (Central)*	45	Baseline	Baseline
Reference	Fast	*Reference (Fast)*	45	x 1.5	x 0.5
Maximum	Slow	*Maximum (Slow)*	71	x 0.5	x 1.5

Maximum	Central	*Maximum (Central)*	71	Baseline	Baseline
Maximum	Fast	*Maximum (Fast)*	71	x 1.5	x 0.5

Table 3: Scenario design matrix mapping the nine modelled scenarios.

3. Results and Discussion

3.1. CGS pathways by geographical participation

Under the *Reference (Central)* scenario, in which countries classified as “Injecting”, “Pipeline” or “Appraised” deploy CGS (Table 2), we see global annual injection reaches 0.14 $GtCO_2yr^{-1}$ by 2030, accelerating to 0.64 $GtCO_2yr^{-1}$ in 2040 and 2.71 $GtCO_2yr^{-1}$ in 2050 (Table 4). Injection peaks at 56.45 $GtCO_2yr^{-1}$ in 2085 (Figure 5).

The *Limited (Central)* and *Maximum (Central)* scenarios produce similar results, with substantial divergence only appearing in the later stages of the modelling period (Figure 5a-b). This is a reflection of both the delayed deployment imposed in our modelling approach to the less-ready countries (Figure 5c) and the dominance of a relatively small group of early-deploying countries common to all three scenarios (Figure 5d). Countries in the “Appraised” or “Conceptual” categories make a significant contribution to global injection only from ~2100 onwards (Figure 5c), reflecting their longer start delays and lower assigned growth rates. Furthermore, the countries at the forefront of CGS deployment, which are included even in the *Limited (Central)* scenario, dominate storage in terms of cumulative volumes, accounting for 89% of total volumes stored even when all 71 countries are modelled (Figure 5d). The full results for all nine scenarios can be found in the Supplementary Data to this article.

Source	Deployment scenario	Parameter	2023	2030	2040	2050	2075	2100	Model end
This study	Limited	Injection rate ($GtCO_2yr^{-1}$)	0.05	0.14	0.64	2.68	46.03	30.76	
		Cumulative ($GtCO_2$)		0.69	4.27	19.68	504.01	1,704.92	2,476.13
	Reference	Injection rate ($GtCO_2yr^{-1}$)	0.05	0.14	0.64	2.71	46.22	31.86	
		Cumulative ($GtCO_2$)		0.69	4.27	19.77	506.60	1,720.82	2,749.75
	Maximum	Injection rate ($GtCO_2yr^{-1}$)	0.05	0.14	0.64	2.71	46.26	31.98	
		Cumulative ($GtCO_2$)		0.69	4.27	19.77	506.72	1,722.96	2,769.59
Actual injection (Gao & Krevor, 2025)		Injection rate ($GtCO_2yr^{-1}$)	0.045						
Total from NDCs (UNFCCC Authors, 2025)		Injection rate ($GtCO_2yr^{-1}$)		0.039[7]					
Feasible rates (Kazlou et al., 2024)		Injection rate ($GtCO_2yr^{-1}$)		0.37[3]	4.3[4]				
Projects under development (IEA, 2026)		Injection rate ($GtCO_2yr^{-1}$)		0.43[8]					

Feasible rates (Zhang et al., 2024)	Maximum rate	Injection rate ($GtCO_2yr^{-1}$)				16[5]			
	Feasible rate	Injection rate ($GtCO_2yr^{-1}$)				5.5[6]			
Pressure-constrained (Smith et al., 2024)		Injection rate ($GtCO_2yr^{-1}$)				26[1]		15[2]	

Table 4: Summary of injection rates from three deployment scenarios with literature values also included for comparison. Note that all values derived from this study reflect the Central scale-up assumption. The superscript numbering refers to annotations shown in Figure 5a.

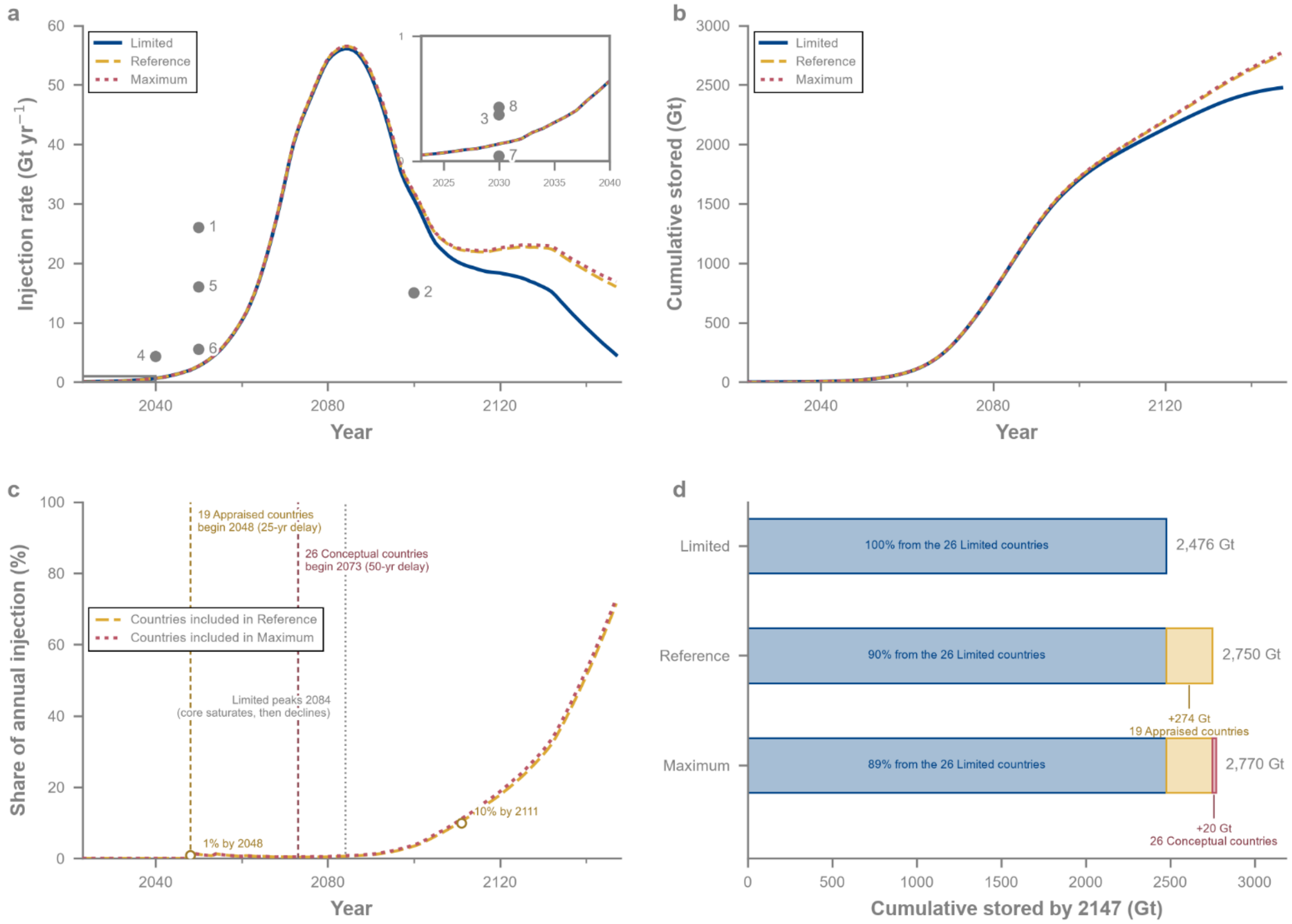

Figure 5: Global injection modelled within three deployment instances. a: modelled injection rates compared against published values with an inset panel illustrating near-term rates up to 2040 and 1 $GtCO_2yr^{-1}$. b: modelled cumulative storage. c: share of injection, over time, from countries outside the Limited set and d: total volumes stored for each set, split by category. The labelled points in panel a refer to published literature values also shown in Table 4. 1-2: Pressure-constrained storage within CCS-ready countries (Smith et al., 2024), 3-4: Upper feasible bounds on CCS capacity (Kazlou et al., 2024), 5: Maximum global storage rate (Zhang et al., 2024), 6: Feasible benchmark (Zhang et al., 2024). 7: Total from Nationally Determined Contributions (UNFCCC Authors, 2025), 8: Planned capacity in projects under development (IEA, 2026)

The results in Figure 5 represent, to our knowledge, the first attempt to couple non-linear growth trajectories in injection activity with global CO_2 storage rates. They also present more conservative near-term estimates than those reported in some other studies. For example, our *Reference (Central)* case estimate for 2030 of 0.14 $GtCO_2yr^{-1}$ exceeds the deployment stated within Nationally Determined Contributions (UNFCCC Authors, 2025) but is lower than the estimates from Kazlou et al. (2024) and the IEA (2026) projection based on projects under development (Figure 5a). The divergence increases over time, with our *Reference (Central)* scenario projecting substantially lower volumes by 2050 than those presented by Smith et al. (2024) and Zhang et al. (2024).

Early CGS deployment is dominated by the USA and Brazil, with smaller contributions from Saudi Arabia, China, Australia, and others (Figure 6). There is relatively little change in countries' proportional contributions until around 2080 (Figure 6c), at which point we see a significant expansion in total storage volumes (Figure 6b) driven mainly by CGS growth in China (Figure 6a, c). Around 20 years later, storage expands in Saudi Arabia, which becomes the highest-ranking country by annual injection rate by 2100 (Figure 6d). By 2120 we see later-adopting countries such as India, Indonesia and Russia dominate the total storage volume, while the contributions of early adopters such as USA and China have waned (Figure 6c-d).

Because near-term and mid-century global injection rates are disproportionately driven by a small group of key nations (the USA and Brazil, followed by China and Saudi Arabia) the global trajectory we model suggests a high policy sensitivity to these specific nations. While we did not undertake a systematic sensitivity analysis to test the impact of suppressing individual high-contributing countries, political or regulatory shifts that disrupt local deployment in these key regions would likely exert significant downward pressure on our projected near-term global growth curves.

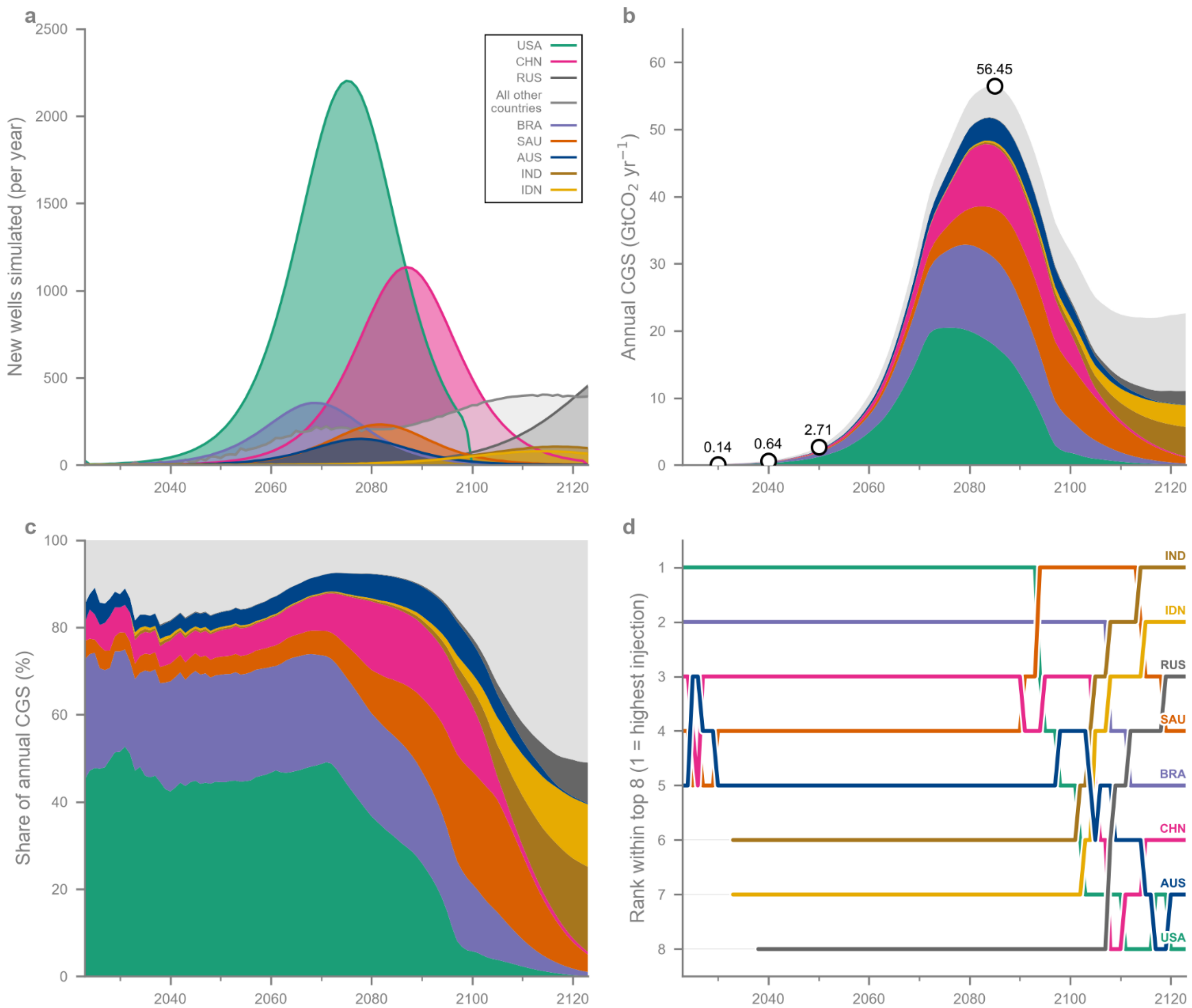

Figure 6: In-depth analysis of the Reference growth scenario with injection rates broken down by country. a: growth curves depicting the new wells scheduled per country per year by the logistic growth model (only eight countries with largest contribution are coloured), b: stacked area plot showing the injection rate per country per year. c: stacked area plot normalised per year to show relative contributions

of each country to the total injected volume, d: line plots depicting the per-country ranking where the country injecting most per year is ranked 1. As with panels a-c, only the top eight ranked countries are shown. Country labels use standard ISO 3-letter codes.

3.2. Impact of scale-up assumptions on CGS pathways

We find substantial variation across scenarios with peak injection rates spanning from 32.6 to 70.9 $GtCO_2yr^{-1}$ and cumulative storage volumes by 2100 ranging from 165.3 to 2,585.3 $GtCO_2$ (Table 5, Figure 7). Almost all this observed variation results from scale-up differences rather than geographic participation. Across the three scale-up rates, the peak injection rate more than doubles, whereas within a given rate, the three deployment scenarios peak within 1.5 $GtCO_2yr^{-1}$ of each other: the *Limited (Central)*, *Reference (Central)* and *Maximum (Central)* scenarios peak at 56.1, 56.4 and 56.5 $GtCO_2yr^{-1}$ in 2084, 2085 and 2085 respectively. This similarity across different deployment scenarios suggests that the global trajectory is driven more by the rate of scale-up than by the number of participating countries.

Under the *Slow* rate, deployment is heavily constrained: "Appraised" countries (Table 2) do not begin injecting until 2060 and "Conceptual" countries (Table 2) until 2098. Injection peaks at 32.6-32.8 $GtCO_2yr^{-1}$ in 2122 then declines to 1.3-1.7 $GtCO_2yr^{-1}$ by 2147 (Table 5, Figure 7). Deployment is so protracted that most participating countries do not reach their midpoint year or maximum growth rate before the end of the simulation timeframe. Consequently, the apparent peak in 2122 and the subsequent sharp drop-off are artefacts of the simulation timeframe; injection rates plummet as active wells reach the end of their 25-year operational lifespans and are not replaced with new ones.

The *Fast* rate has the opposite effect, resulting in both earlier and greater peak injection rates. Under *Fast* scale-up assumptions, the three deployment scenarios peak in 2070, at 69.4 (*Limited*), 70.7 (*Reference*) and 70.9 $GtCO_2yr^{-1}$ (*Maximum*) - 14 to 15 years earlier and roughly a quarter higher than under the central rate (Table 5, Figure 7). Halving the assigned delays brings "Appraised" countries into the model in 2035 and "Conceptual" countries in 2048, allowing these later-adopting countries to begin injecting CO_2 while the early adopters are still growing. The arrival of these later adopters appears as a shoulder on the descending limb, most clearly under *Maximum (Fast)*, where injection plateaus between 2090 and 2104 before resuming its decline (Figure 7). The same feature appears at *Reference (Central)* and *Maximum (Central)* scenarios which plateau between 2108 and 2135 and remain at 28% and 30% of their respective peaks at 2147, whereas *Limited (Central)* has fallen to 8% by that point.

The interaction between scale-up rate and geographic participation is strongly asymmetric. Under the *Slow* rate, widening participation has a negligible effect: cumulative storage by 2147 rises only from 1,101.4 $GtCO_2$ under *Limited (Slow)* to 1,115.8 $GtCO_2$ under *Maximum (Slow)*, an increase of 1.3%. This is because the additional countries do not begin injecting until 2060 or 2098 and have too little of the simulation period remaining to scale substantially. The same widening of participation (from *Limited* to *Maximum)* adds a much more significant 293.5 $GtCO_2$ (11.9%) at the *Central* rate and 999.5 $GtCO_2$ (38.3%) at the *Fast* rate. Geographical participation therefore only delivers substantial additional storage where the scale-up rate is high enough for late-starting countries to grow within the simulation timeframe.

Pressure-related well shut-in also varies substantially across deployment scenarios, rising sharply with the pace of deployment. Under the *Limited (Slow)* scenario, 2,225 of the approximately 41,400-42,000 simulated wells reach the pressure limit and are thus shut in before the simulation ends, corresponding to 1.7 $GtCO_2$ of capacity that would otherwise be stored ("lost capacity") (Table 6). However, under the *Reference (Central)* scenario, curtailment increases substantially: 12,192 of 152,523 simulated wells globally (8.0%) are shut in before the end of their nominal 25-year lifespan, corresponding to a lost capacity of 20.8 $GtCO_2$ (Table 6). This curtailment is concentrated within a small number of important storage nations: the USA alone accounts for 7,027 shut-in wells and 10.8 $GtCO_2$ of lost capacity (52% of the global total), with China a distant second (2,463 wells, 5.7 $GtCO_2$). Both are countries central to the early deployment of CGS (Figure 6), suggesting that the same rapid, geographically limited growth also brings local pressure challenges. Under faster scale-up rates, the number of wells shut in rises further to 17,637 (*Reference (Fast)*) and 17,747 (*Maximum (Fast)*), with up to 33.6 $GtCO_2$ of lost capacity; Libya (664 wells, 3.8 $GtCO_2$) and Russia (3,188 wells, 2.8 $GtCO_2$) join the USA and China among the most heavily affected countries. This premature well shut-in reduces the effective utilisation of injection infrastructure, implying that achieving a given level of climate mitigation through CGS may require greater infrastructure deployment and associated investment.

Expressed as a proportion of the wells deployed, well shut-ins track the scale-up rate rather than the number of countries participating, rising from 5.3-5.4% under *Slow* scenarios to 7.9-8.6% under *Central* scenarios and 9.2-10.5% under *Fast* scenarios (Table 6). Within a given rate, the proportion falls slightly as country participation widens, from 10.5% under *Limited (Fast)* to 9.2% under *Maximum (Fast)*. This is because the countries added in the scenarios with wider participation deploy at low intensity and rarely reach their pressure limits: between 93% and 100% of shut-in wells, and approximately 95-100% of lost capacity occur in the Injecting and Pipeline countries (Table 2) common to every scenario. This suggests that these pressure-related constraints are controlled by the pace of deployment within today's leading storage nations, rather than by geographical participation.

Deployment scenario	Scale-up assumption	Peak injection rate ($GtCO_2yr^{-1}$)	Year of peak injection rate	Stored by 2100 ($GtCO_2$)
Limited	Slow	32.6	2122	165.3
	Central	56.1	2084	1,704.9
	Fast	69.4	2070	2,362.4
Reference	Slow	32.7	2122	167.5
	Central	56.4	2085	1,720.8
	Fast	70.7	2070	2,566.0
Maximum	Slow	32.8	2122	167.6
	Central	56.5	2085	1,723.0
	Fast	70.9	2070	2,585.3

Table 5: Summary of outputs from different deployment and scale-up scenarios.

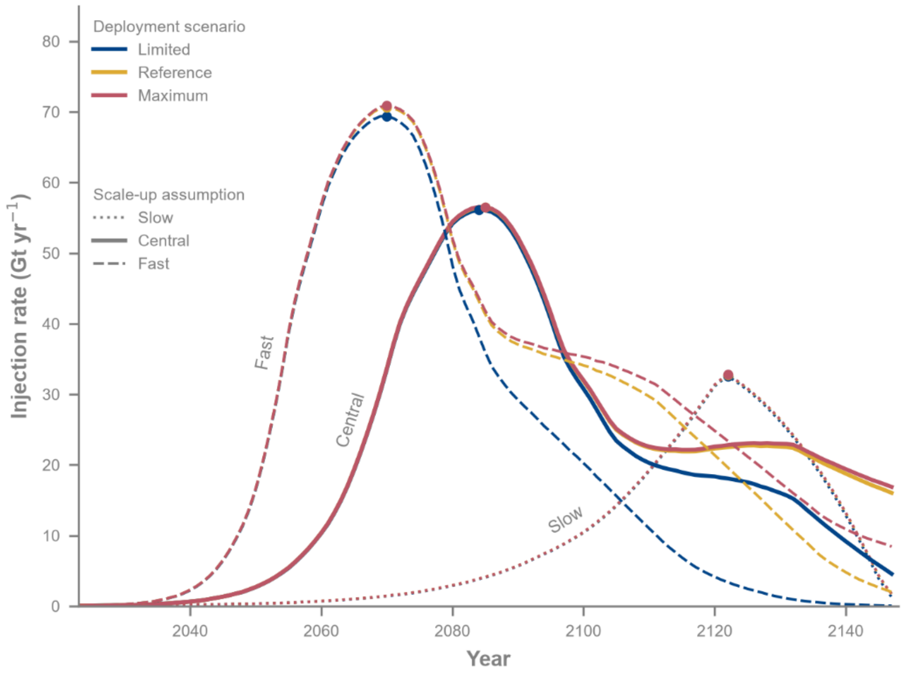

Figure 7: Summary of annual injection modelled for each deployment (denoted by colour) and scale-up (denoted by line styling) scenario. Peak injection rates are marked by circles.

Deployment scenario	Scale-up assumption	Total wells	Wells shut-in	Proportion of wells shut-in (%)	Capacity lost due to shut-in wells ($GtCO_2$)
Limited	Slow	41,420	2,225	5.4	1.7
	Central	141,234	12,124	8.6	20.8
	Fast	157,619	16,572	10.5	31.8
Reference	Slow	41,876	2,225	5.3	1.7
	Central	152,523	12,192	8	20.8
	Fast	183,427	17,637	9.6	33.6
Maximum	Slow	41,953	2,225	5.3	1.7
	Central	153,393	12,192	7.9	20.8
	Fast	192,167	17,747	9.2	33.6

Table 6: Wells shut-in and capacity lost where local pressure limits are reached per deployment scenario and scale-up assumption.

3.3. Implications for climate change mitigation projections

According to projections published in the IPCC AR6 Scenario Explorer, CGS deployment could peak at 36 $GtCO_2yr^{-1}$ if global warming is to be limited to 1.5°C by 2100, although the median across these pathways is substantially lower, at 14.5 $GtCO_2yr^{-1}$ (Byers et al., 2022). This translates to a maximum cumulative storage requirement of 1,788 $GtCO_2$, substantially below many accounts of potential maximum available geological storage potential globally.

We find that, in cumulative storage terms, scale-up rate strongly influences how simulated CGS deployment in this study compares with such pathways. Estimates from our model span 165.3 to 2,585.3 $GtCO_2$ stored by 2100 (Figure 8a). For *Central* scale-up rate scenarios, CO2LOGIX stores 1,704.9-1,723.0 $GtCO_2$ by 2100, exceeding 99% of C1 pathways and approaching the single most CGS-intensive pathway in the AR6 database. At the *Fast* rate, 2,362.4-2,585.3 $GtCO_2$ exceeds every C1 pathway by a significant margin. However, for *Slow* scale-up rate scenarios, cumulative storage of 165.3-167.6 $GtCO_2$ falls short of almost all C1 projections, exceeding just 2% of pathways (Figure 8a).

The divergence between C1 scenarios and CO2LOGIX outputs is greater when comparing annual injection rates rather than cumulative storage (Figure 8b). By 2030 the median IPCC C1 pathway deploys 1.11 $GtCO_2yr^{-1}$ – approximately eight times the 0.14 $GtCO_2yr^{-1}$ produced by our *Reference (Central)* scenario – and this gap persists through mid-century (7.82 $GtCO_2yr^{-1}$ for the C1 median versus 2.71 $GtCO_2yr^{-1}$ for CO2LOGIX 2.0 in 2050). Importantly, this near-term shortfall is not driven by conservative growth assumptions – even under the *Reference (Fast)* scenario, CO2LOGIX only reaches 0.25 $GtCO_2yr^{-1}$ by 2030, less than one quarter of the C1 median.

Scale-up rate strongly influences when this relationship reverses and the magnitude of the subsequent divergence (Figure 8c). Our *Reference (Central)* trajectory does not overtake the IAM median until 2060 (Figure 8c), after which the relationship reverses and CO2LOGIX 2.0 projects progressively higher injection rates, reaching two to four times the IAM median in the second half of the century and peaking at approximately four times the median in 2083. Our *Reference (Fast)* scenario overtakes the IAM median 15 years earlier, in 2045, and the overshoot reaches six times the median by 2063. For the *Reference (Slow)* scenario, the trajectory never reaches parity with the IAM trajectories, reaching just 0.7 times the IAM median by 2100.

The divergence likely reflects fundamental differences in the trajectory of deployment, together with the many endogenous economic, policy and energy-system processes that IAMs represent but that CO2LOGIX 2.0 does not. The comparison suggests that near-term IAM projections may front-load CGS to satisfy cost-optimal emissions budgets at rates that are not reproduced by our drilling- and pressure-limited growth trajectories. Over the longer term, however, these constraints can accommodate a substantially expanded industry in the absence of other limiting factors. Resolving this discrepancy will require integrating physical deployment constraints with the economic and policy dynamics represented in IAMs.

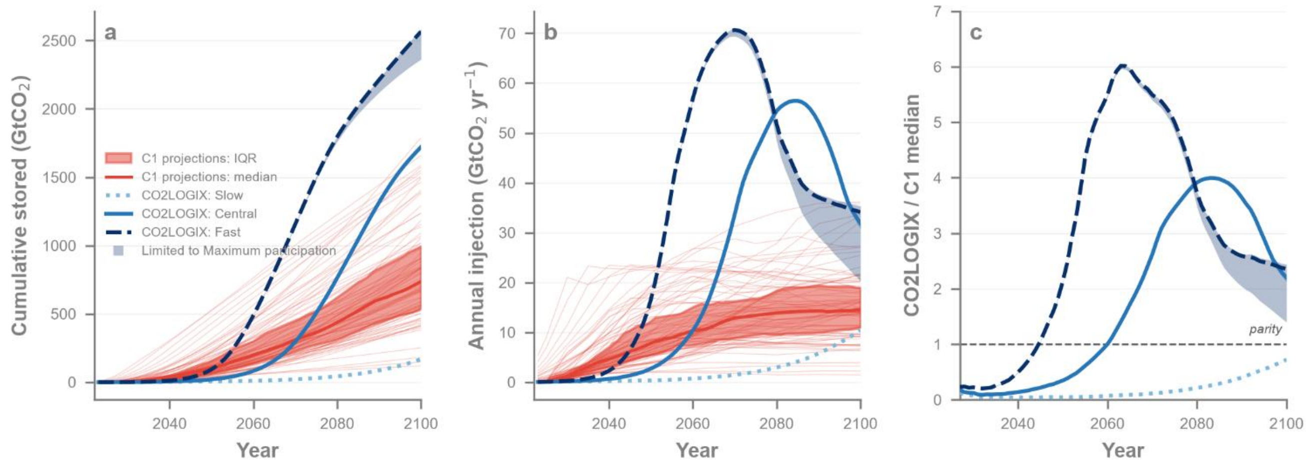

Figure 8: Comparison of CO2LOGIX estimates with CGS projections in the IPCC AR6 database. We only include climate change mitigation scenarios that result in 1.5 °C global warming by 2100 with no or limited overshoot. Lines show the three scale-up rates under Reference deployment, while blue shading spans the Limited to Maximum deployment scenarios for each scale-up rate (only wide enough to be visible for the fast scale-up scenario). a: cumulative injection; b: annual injection; and c: ratio of modelled annual injection to the C1 ensemble median. The dashed line marks parity; values below indicate slower deployment in CO2LOGIX than in the median IAM pathway, whereas values above indicate faster deployment.

3.4. Where untapped storage potential exists

Across the nine modelling scenarios we run (Table 3), cumulative storage utilises between 28% and 92% of the 3,935 $GtCO_2$ assessed global storage resource (Table 7). Even under the *Maximum (Fast)* scenario 324 $GtCO_2$ (8%) of capacity remains untapped at the end of the simulation. Under the *Reference (Central)* scenario, 30% of global capacity (1,185 $GtCO_2$) is not accessed, of which 725 $GtCO_2$ lies within countries that do deploy and 460 $GtCO_2$ in countries that do not initiate deployment (i.e. are not added to the model).

Under the *Slow* scale-up scenarios, the untapped share remains approximately 72% irrespective of how many countries participate, since deployment is too protracted for wider participation to have any meaningful impact within the simulated timeframe. At the opposite extreme, the *Limited (Fast)* exhausts 99% of the capacity available to its 26 deploying countries, leaving just 37 $GtCO_2$ untapped within them. Here, scale-up is not the binding constraint; instead, further global storage requires deployment to expand into additional countries.

Deployment scenario	Scale-up assumption	Total stored		Remaining (in countries deploying)		Remaining (in countries not deploying)		Utilised (in deployed countries) (%)
		Stored ($GtCO_2$)	%	Storage ($GtCO_2$)	%	Storage ($GtCO_2$)	%	
Limited	Slow	1101	28	1548	39	1286	33	42
	Central	2476	63	173	4	1286	33	93
	Fast	2612	66	37	1	1286	33	99
Reference	Slow	1113	28	2362	60	460	12	32
	Central	2750	70	725	18	460	12	79
	Fast	3403	86	72	2	460	12	98
Maximum	Slow	1116	28	2820	72	0	0	28
	Central	2770	70	1166	30	0	0	70
	Fast	3612	92	324	8	0	0	92

Table 7: Summary of the proportion of global storage resource utilised and remaining at the end of each scenario.

The distribution of untapped potential is consistent across scenarios and reveals two distinct responses to increasing scale-up rates (Figure 9).

The first group responds strongly as scale-up rates increase. India falls from 97% untapped under *Maximum (Slow)* to 21% under *Maximum (Central)* and 1% under *Maximum (Fast)*, with Iran, Nigeria, Kazakhstan, Russia, and the Southeast Asian storage hubs of Indonesia and Malaysia following the same pattern (Figure 9). In these countries, storage potential is efficiently utilised once deployment scales, leaving limited additional storage to be unlocked through further development incentives. The effect is widespread: under *Maximum (Fast)*, 45 of the 71 countries (holding 3,475 $GtCO_2$ of storage resource between them) are more than 90% utilised.

The second group remains substantially untapped in every scenario, even under the most ambitious combination of deployment and scale-up. Under the *Reference (Central)* scenario, 26 countries holding 460 $GtCO_2$ (12% of global storage potential) do not initiate deployment at all, as they fall within the “Conceptual” class and are excluded from that scenario. These include Iraq (90 $GtCO_2$), Senegal (74 $GtCO_2$), Argentina (62 $GtCO_2$) and Tanzania (42 $GtCO_2$). Critically, these countries remain largely unused even under the *Maximum*

(Fast) scenario, in which all 71 countries deploy at the fastest rate considered: Argentina retains 87% of its storage potential, Iraq 71%, Senegal 67%, Turkmenistan 56%, Tanzania 55% and Bolivia 54%. These six countries, combining to 287 $GtCO_2$ storage potential (7% of the global total), are still more than half untapped even under the most aggressive scenario we model, because deployment begins too late in the simulation period for their storage industries to scale sufficiently. Here, the binding constraint is the timing of country-level initiation rather than either geological capacity or subsequent scale-up. These countries therefore represent potential targets for policy stimulus, whereas support directed at the first group would be expected to deliver comparatively smaller gains in storage utilisation. Such targeted support could also help reduce emerging inequalities in CGS development, by enabling storage-rich but less-ready countries to develop alongside established CGS regions rather than allowing existing disparities in readiness and capability to widen (Alcalde et al., 2025). Overall, these results suggest that maximising global geological storage utilisation depends less on the magnitude of the assessed resource than on the timing and geographical expansion of CGS deployment.

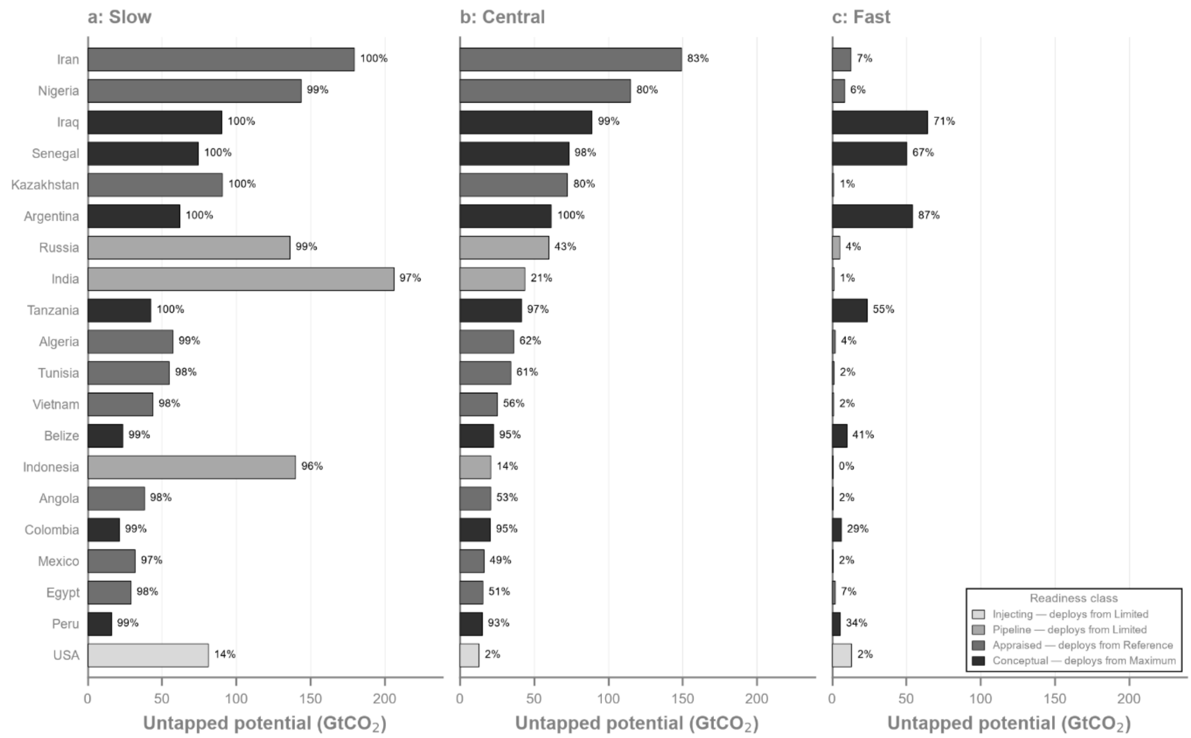

Figure 9: Untapped storage potential per country under the three scale-up rate assumptions modelled (a: Slow, b: Central, c: Fast). All three panels use Maximum deployment, allowing all countries to be compared. Bar length is the assessed pressure-limited storage capacity that remains untapped at the end of the simulation, and the adjacent label shows this volume as a percentage of the country's own storage potential. Only the 20 countries with the largest untapped storage potential are shown, ranked by their untapped volume under the central rate and held in that order across all three panels to allow comparison. Bar shading denotes readiness class (Table 2), and the legend states the least ambitious deployment scenario in which each class begins injecting.

4. Conclusions

In this study we present the first global assessment of pressure-constrained CO_2 storage deployment. We use CO2LOGIX 2.0 to couple subsurface pressure evolution with country-level logistic growth trajectories, informed by historical drilling rates, project pipelines, storage readiness indicators and injection volumes to date. We model nine scenarios to explore two dimensions of future growth: the geographical participation of deployment and the rate at which participating countries scale their storage industries.

Our *Reference (Central)* scenario suggests that near-term global injection rates will be significantly lower than existing feasibility estimates, reaching only 2.71 $GtCO_2yr^{-1}$ by 2050. Over the longer term the industry scales to a peak of 56.45 $GtCO_2yr^{-1}$ in 2085 – corresponding to 1,720.8 $GtCO_2$ of storage by 2100 - a volume exceeding all but the most storage-intensive Integrated Assessment Model pathways that limit warming to 1.5 °C, and more than double the ensemble median. The shape of the trajectory differs sharply between our model and IAMs, however: IAMs project early-stage growth that our drilling-rate-informed modelling suggests is unlikely to materialise, deploying eight times our Reference rate by 2030, while even our most aggressive assumptions fall more than fourfold short. By contrast, under slow growth the gap never closes, with 167.5 $GtCO_2$ stored by 2100, below almost every projection.

Scale-up assumptions we model have the strongest influence on the timing and magnitude of peak global injection: across the three scale-up assumptions, peak injection more than doubles and arrives up to 52 years earlier, whereas widening participation from 26 to 71 countries changes the peak rate by less than 1% at our central scale-up rate. Geographical participation becomes increasingly important over longer timescales, however, particularly when rapid scale-up allows later-adopting countries sufficient time to grow their CGS deployment within the timeframe we simulate. In our model, deployment is initially concentrated in early adopters such as the USA and Brazil, before later expansion within China, Saudi Arabia, India and Southeast Asia; sustained gigatonne-scale storage through the latter half of the century therefore depends on substantial geographic diversification beyond today's leading nations.

Global geological storage capacity does not emerge as the limiting factor for any scenario, with cumulative storage utilising between 28% and 92% of the 3,935 $GtCO_2$ of pressure-constrained storage capacity. Even under the most aggressive growth assumptions, 324 $GtCO_2$ (8%) of potential storage resource remains untapped, rising to 30% under our *Reference (Central)* scenario. This untapped storage potential is concentrated in sub-Saharan Africa, the Middle East and South America, particularly in countries where deployment either never initiates or stalls at low levels irrespective of global ambition. The binding constraint on global storage is thus not geological capacity but country-level initiation, indicating that policy support targeted at these regions would unlock more additional storage than further stimulus of markets that scale regardless.

Ultimately, CO2LOGIX 2.0 provides an adaptable, data-driven framework for bridging the gap between theoretical geological potential and the pragmatic realities of CGS deployment and scale-up, and its outputs offer a physically grounded constraint for the storage assumptions embedded in climate mitigation pathways.

5. Acknowledgements

IdJA and JJR received funding from the European Union's Horizon Europe research and innovation programme under grant agreement No 101081521 - UPTAKE - Bridging current knowledge gaps to enable the UPTAKE of carbon dioxide. Contains information provided by the North Sea Transition Authority and/or other third parties.

Declaration of generative AI and AI-assisted technologies in the manuscript preparation process

During the preparation of this work the authors used Claude in order to highlight spelling, grammar and sentence structure improvements. After using this tool, the authors reviewed and edited the content as needed and take full responsibility for the content of the published article.

6. References

Alcalde, J., Johnson, G., & Roberts, J. J. (2025). National climate strategies show inequalities in global development of carbon dioxide geological storage. *Communications Earth & Environment*, *6*(1), 61. https://doi.org/10.1038/s43247-025-02043-4

Bachu, S. (2015). Review of CO_2 storage efficiency in deep saline aquifers. *International Journal of Greenhouse Gas Control*, *40*, 188-202. https://doi.org/10.1016/j.ijggc.2015.01.007

Birkholzer, J. T., & Zhou, Q. (2009). Basin-scale hydrogeologic impacts of CO_2 storage: Capacity and regulatory implications. *International Journal of Greenhouse Gas Control*, *3*(6), 745-756. https://doi.org/10.1016/j.ijggc.2009.07.002

Bump, A. P., Bakhshian, S., Ni, H., Hovorka, S. D., Olariu, M. I., Dunlap, D., Hosseini, S. A., & Meckel, T. A. (2023). Composite confining systems: Rethinking geologic seals for permanent CO2 sequestration. *International Journal of Greenhouse Gas Control*, *126*, 103908. https://doi.org/10.1016/j.ijggc.2023.103908

Bump, A. P., & Hovorka, S. D. (2024). Pressure space: The key subsurface commodity for CCS. *International Journal of Greenhouse Gas Control*, *136*, 104174. https://doi.org/10.1016/j.ijggc.2024.104174

Byers, E., Krey, V., Kriegler, E., Riahi, K., Schaeffer, R., Kikstra, J., Lamboll, R., Nicholls, Z., Sandstad, M., Smith, C., van der Wijst, K., Al - Khourdajie, A., Lecocq, F., Portugal-Pereira, J., Saheb, Y., Stromman, A., Winkler, H., Auer, C., Brutschin, E.,...van Vuuren, D. (2022). *AR6 Scenarios Database* (Integrated Assessment Modeling Consortium & International Institute for Applied Systems Analysis. https://doi.org/10.5281/ZENODO.7197970

Consoli, C. (2018). *CCS Storage Indicator (CCS-SI)*. https://www.globalccsinstitute.com/wp-content/uploads/2020/04/CCS-Storage-Indicator-CCS-SI-DIGITAL-1.pdf

de Jonge-Anderson, I., Johnson, G., Alcalde, J., & Roberts, J. J. (2026). CO2LOGIX: A first-order model of pressure-constrained CO_2 geological storage growth at the basin scale. *International Journal of Greenhouse Gas Control*, *151*, 104608. https://doi.org/10.1016/j.ijggc.2026.104608

De Luca, M., Mackay, E. J., Good, T. R., Scisciani, V., MacBeth, C., Patruno, S., & Sutcliffe, J. (2025). Regional pressure response to large-scale carbon storage in the bunter sandstone formation, Silverpit Basin (Southern North Sea, UK). *International Journal of Greenhouse Gas Control*, *148*, 104530. https://doi.org/10.1016/j.ijggc.2025.104530

De Simone, S., Jackson, S. J., & Krevor, S. (2019). The Error in Using Superposition to Estimate Pressure During Multisite Subsurface CO_2 Storage. *Geophysical Research Letters*, *46*(12), 6525-6533. https://doi.org/10.1029/2019gl082738

De Simone, S., & Krevor, S. (2021). A tool for first order estimates and optimisation of dynamic storage resource capacity in saline aquifers. *International Journal of Greenhouse Gas Control*, *106*, 103258. https://doi.org/10.1016/j.ijggc.2021.103258

Edwards, M. R., Thomas, Z. H., Nemet, G. F., Rathod, S., Greene, J., Surana, K., Kennedy, K. M., Fuhrman, J., & McJeon, H. C. (2024). Modeling direct air carbon capture and storage in a 1.5 °C climate future using historical analogs. *Proceedings of the National Academy of Sciences*, *121*(20), e2215679121. https://doi.org/10.1073/pnas.2215679121

Evenick, J. C. (2021). Glimpses into Earth's history using a revised global sedimentary basin map. *Earth-Science Reviews*, *215*, 103564. https://doi.org/10.1016/j.earscirev.2021.103564

Fuhrman, J., Lane, J., McJeon, H., Iyer, G. C., Edwards, M. R., Thomas, Z., & Edmonds, J. A. (2025). Rate and growth limits for carbon capture and storage. *Environmental Research Letters*, *20*(6), 064034. https://doi.org/10.1088/1748-9326/add9af

Gao, X., & Krevor, S. (2025). *The London Register of Subsurface CO_2 Storage* (https://doi.org/10.5281/zenodo.18016847

Gidden, M. J., Joshi, S., Armitage, J. J., Christ, A.-B., Boettcher, M., Brutschin, E., Köberle, A. C., Riahi, K., Schellnhuber, H. J., Schleussner, C.-F., & Rogelj, J. (2025). A prudent planetary limit for geologic carbon storage. *Nature*, *645*(8079), 124-132. https://doi.org/10.1038/s41586-025-09423-y

Goodman, A., Hakala, A., Bromhal, G., Deel, D., Rodosta, T., Frailey, S., Small, M., Allen, D., Romanov, V., Fazio, J., Huerta, N., McIntyre, D., Kutchko, B., & Guthrie, G. (2011). U.S. DOE methodology for the development of geologic storage potential for carbon dioxide at the national and regional scale. *International Journal of Greenhouse Gas Control*, *5*(4), 952-965. https://doi.org/https://doi.org/10.1016/j.ijggc.2011.03.010

Hansen, O., Gilding, D., Nazarian, B., Osdal, B., Ringrose, P., Kristoffersen, J.-B., Eiken, O., & Hansen, H. (2013). Snøhvit: The History of Injecting and Storing 1 Mt CO2 in the Fluvial Tubåen Fm. *Energy Procedia*, *37*, 3565-3573. https://doi.org/10.1016/j.egypro.2013.06.249

Hendriks, C., Graus, W., & Van Bergen, F. (2004). *Global Carbon Dioxide Storage Potential and Costs*. http://inis.iaea.org/search/search.aspx?orig_q=RN:35053050

IEA. (2025). *World Energy Outlook 2025*. https://www.iea.org/reports/world-energy-outlook-2025

IEA. (2026). *CCUS Projects Database* (https://www.iea.org/data-and-statistics/data-product/ccus-projects-database

Kazlou, T., Cherp, A., & Jewell, J. (2024). Feasible deployment of carbon capture and storage and the requirements of climate targets. *Nature Climate Change*, *14*(10), 1047-1055. https://doi.org/10.1038/s41558-024-02104-0

Kivi, I. R., De Simone, S., & Krevor, S. (2025). A simplified physics model for estimating subsurface CO_2 storage resources constrained by fault slip potential. *Journal of Rock Mechanics and Geotechnical Engineering*. https://doi.org/10.1016/j.jrmge.2025.06.031
Lane, J., Greig, C., & Garnett, A. (2021). Uncertain storage prospects create a conundrum for carbon capture and storage ambitions. *Nature Climate Change*, *11*(11), 925-936. https://doi.org/10.1038/s41558-021-01175-7
Nemet, G., Greene, J., Müller-Hansen, F., & Minx, J. C. (2023). Dataset on the adoption of historical technologies informs the scale-up of emerging carbon dioxide removal measures. *Communications Earth & Environment*, *4*(1), 397. https://doi.org/10.1038/s43247-023-01056-1
Newman, G. H. (1973). Pore-Volume Compressibility of Consolidated, Friable, and Unconsolidated Reservoir Rocks Under Hydrostatic Loading. *Journal of Petroleum Technology*, *25*(02), 129-134. https://doi.org/10.2118/3835-PA
Nordbotten, J. M., Celia, M. A., & Bachu, S. (2005). Injection and Storage of CO_2 in Deep Saline Aquifers: Analytical Solution for CO_2 Plume Evolution During Injection. *Transport in Porous Media*, *58*(3), 339-360. https://doi.org/10.1007/s11242-004-0670-9
NSTA. (2024). *NSTA awards Endurance first ever UK carbon storage permit*. Retrieved 9th July 2026 from https://www.nstauthority.co.uk/news-publications/nsta-awards-endurance-first-ever-uk-carbon-storage-permit/
Okwen, R. T., Stewart, M. T., & Cunningham, J. A. (2010). Analytical solution for estimating storage efficiency of geologic sequestration of CO2. *International Journal of Greenhouse Gas Control*, *4*(1), 102-107. https://doi.org/10.1016/j.ijggc.2009.11.002
Pett-Ridge, J., Kuebbing, S., Mayer, A. C., Hovorka, S., Pilorgé, H., Baker, S. E., Pang, S. H., Scown, C. D., Mayfield, K. K., Wong, A. A., Aines, R. D., Ammar, H. Z., Aui, A., Ashton, M., Basso, B., Bradford, M., Bump, A. P., Busch, I., Calzado, E. R.,...Zhang, Y. (2023). *Roads to Removal: Options for Carbon Dioxide Removal in the United States*. https://www.osti.gov/servlets/purl/2301853
Ringrose, P. S., & Meckel, T. A. (2019). Maturing global CO_2 storage resources on offshore continental margins to achieve 2DS emissions reductions. *Scientific Reports*, *9*(1), 17944. https://doi.org/10.1038/s41598-019-54363-z
Shi, J.-Q., Durucan, S., Korre, A., Ringrose, P., & Mathieson, A. (2019). History matching and pressure analysis with stress-dependent permeability using the In Salah CO_2 storage case study. *International Journal of Greenhouse Gas Control*, *91*, 102844. https://doi.org/10.1016/j.ijggc.2019.102844
Smith, A., Hampson, G., Kivi, I. R., & Krevor, S. (2025). Carbon dioxide plumes, pressure space and legacy well risk for Southern North Sea CO2 Storage Projects. *Energy Geoscience*, 100475. https://doi.org/10.1016/j.engeos.2025.100475
Smith, A., Hampson, G., & Krevor, S. (2024). Global analysis of geological CO_2 storage by pressure-limited injection sites. *International Journal of Greenhouse Gas Control*, *137*, 104220. https://doi.org/10.1016/j.ijggc.2024.104220
Thibeau, S., & Adler, F. (2023). Pressure-derived storage efficiency for open saline aquifer CO_2 storage. *Geoenergy*, *1*(1), geoenergy2022-2003. https://doi.org/10.1144/geoenergy2022-003
Thibeau, S., Bachu, S., Birkholzer, J., Holloway, S., Neele, F., & Zhou, Q. (2014). Using Pressure and Volumetric Approaches to Estimate CO_2 Storage Capacity in Deep Saline Aquifers. *Energy Procedia*, *63*, 5294-5304. https://doi.org/10.1016/j.egypro.2014.11.560
UNFCCC Authors. (2025). *Additional information on domestic mitigation measures. 2025*. https://unfccc.int/documents/650854
Valluri, M., Mishra, S., & Ravi Ganesh, P. (2021). Injectivity index: a powerful tool for characterizing CO_2 storage reservoirs—a technical note. *Greenhouse Gases: Science and Technology*, *11*(2), 251-265. https://doi.org/https://doi.org/10.1002/ghg.2046
van der Meer, L. G. H. (1995). The CO2 storage efficiency of aquifers. *Energy Conversion and Management*, *36*(6), 513-518. https://doi.org/10.1016/0196-8904(95)00056-J
Waring, T., & Longo, A. (2025). Implementing Carbon Capture and Storage in the United Kingdom: Estimating Willingness to Pay through a Contingent Valuation Survey. *Environmental Management*, *75*(6), 1432-1443. https://doi.org/10.1007/s00267-025-02174-6
Wei, Y.-M., Kang, J.-N., Liu, L.-C., Li, Q., Wang, P.-T., Hou, J.-J., Liang, Q.-M., Liao, H., Huang, S.-F., & Yu, B. (2021). A proposed global layout of carbon capture and storage in line with a 2 °C climate target. *Nature Climate Change*, *11*(2), 112-118. https://doi.org/10.1038/s41558-020-00960-0
Worden, R. H. (2024). Carbon Dioxide Capture and Storage (CCS) in Saline Aquifers versus Depleted Gas Fields. *Geosciences*, *14*(6), 146. https://doi.org/10.3390/geosciences14060146
ZEP. (2010). *Moving forward with CO2 Capture and Storage (CCS)*. https://carbonmanagementeurope.org/publication/moving-forward-with-co2-capture-and-storage-ccs/
Zhang, J., & Yin, S.-X. (2017). Fracture gradient prediction: an overview and an improved method. *Petroleum Science*, *14*(4), 720-730. https://doi.org/10.1007/s12182-017-0182-1
Zhang, Y., Jackson, C., & Krevor, S. (2024). The feasibility of reaching gigatonne scale CO_2 storage by mid-century. *Nature Communications*, *15*(1), 6913. https://doi.org/10.1038/s41467-024-51226-8

7. Appendices

We estimated upper bounds on static, global storage potential. Previous studies harnessing global scale geospatial datasets have estimated storage potential to range between ~1,500 $GtCO_2$ and 3,500 $GtCO_2$ (Gidden et al., 2025; Hendriks et al., 2004; Wei et al., 2021). These studies typically derive storage capacity from geometric and petrophysical characteristics of sedimentary formations and use screening methodologies to identify suitable regions for developing CGS. Here, we adopt three approaches to determining static storage potential, i.e. storage potential that does not account for subsurface or site development dynamics. It is important to emphasise that we only consider a subset of available storage options: saline aquifer storage across

203 sedimentary basins. We do not consider storage in hydrocarbon fields (depleted or producing) or mafic mineralisation.

As a first estimate we calculate a theoretical maximum corresponding to the mass of CO_2, under subsurface pressure and temperature conditions, that can be stored within the entire porous volume of sedimentary aquifers globally (Table A1). Following this, we consider the fraction of porous rock volume that might practically be accessible to CO_2 (volumetric displacement) by introducing a storage efficiency factor. While storage efficiency factors (Bachu, 2015; Goodman et al., 2011; Okwen et al., 2010; Thibeau & Adler, 2023; van der Meer, 1995) often implicitly include some degree of pressure constraints, they primarily represent the volume of native brine that can be displaced by CO_2. We adopt a range of estimates - 0.012, 0.024 and 0.041 - based on the work of Bachu (2015). Applying these to the global pore volume factors results in an estimated range of 3,138 $GtCO_2$ to 10,721 $GtCO_2$ (Table A1).

Estimate type	Method	Low ($GtCO_2$)	Medium ($GtCO_2$)	High ($GtCO_2$)
Theoretical maximum	$A \times h \times \varphi \times \rho$	261,495		
Volumetric displacement	$A \times h \times \varphi \times \rho \times \varepsilon$	3,138	6,276	10,721
Pressure-space	$A \times h \times \varphi \times \rho \times C \times \Delta P$	2,595	3,935	5,276

Table A1: Summary of geological storage potential upper bounds. *This table summarises the global estimates using three different methods. "Theoretical maximum" assumes all pore space can be filled with CO_2. "Volumetric displacement" introduces a storage efficiency factor to represent how much pore space might be feasibly accessible. We use factors of 0.012 (low), 0.024 (medium) and 0.041 (high) respectively. "Pressure-space" assumes the same pore volume can be entirely pressured to a given pressure limit, and we adopt low, medium and high pressure limits of 70%, 80% and 90% of fracture pressure respectively.*

Thirdly, we adopt the methodology of Bump and Hovorka (2024), which conceptualises the subsurface as a closed system where capacity is a function of elastic compression rather than displacement (pressure-space). For this, we estimate pore volume compressibility from porosity using the Newman (1973) empirical equation for consolidated sandstones. We assume three risk tolerances for pressure limits and derive three global estimates: low (70% of fracture pressure), medium (80% of fracture pressure) and high (90% of fracture pressure) and find that geological storage potential under these conditions ranges from 2,595 $GtCO_2$ to 5,276 $GtCO_2$ (Table A1). This storage potential is distributed unevenly, concentrated primarily in the USA, Brazil and Saudi Arabia (Figure A1e-f).

Moving forward, we adopt the medium pressure-constrained storage potential of 3,935 $GtCO_2$ as our upper bound. This forms a key input parameter for CO2LOGIX, as it informs the carrying capacity of a country's logistic growth curve (where carrying capacity is the theoretical maximum number of injection wells required to fully exhaust this storage potential).

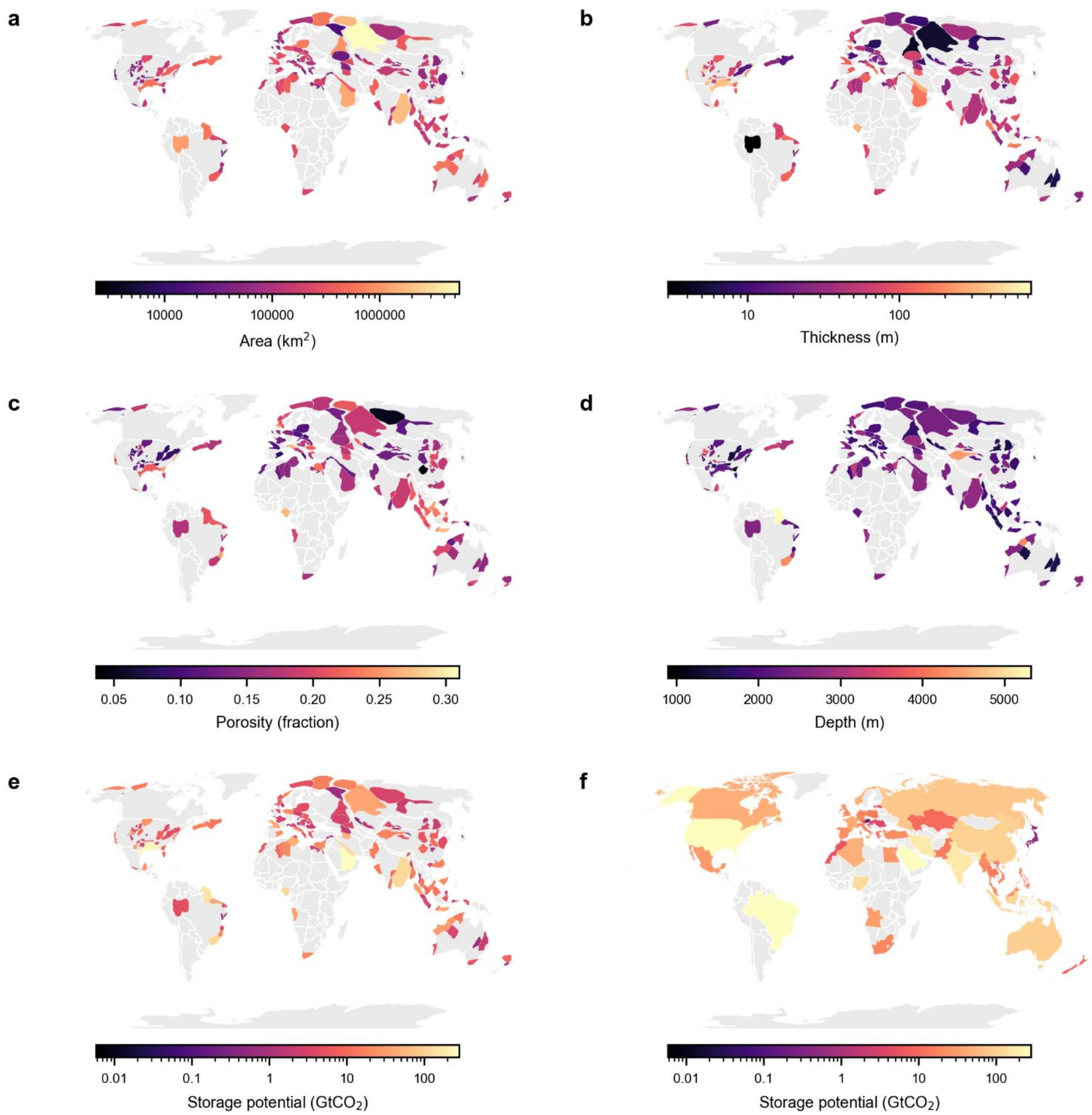

Figure A1: World maps depicting per-basin geological properties and storage capacity. a: basin area, b: average thickness of saline aquifer, c: average porosity of saline aquifer, d: average depth of saline aquifer, e: storage potential per basin and f: aggregated storage potential per country. Storage potential per basin (e) is calculated using the methodology of Bump and Hovorka (2024) as outlined in de Jonge-Anderson et al. (2026). The underlying input data is primarily from Smith et al. (2024), with the exception of the UK and USA which are taken from de Jonge-Anderson et al. (2026) and Pett-Ridge et al. (2023) respectively.